



Human Alpha-Aminoadipic Semialdehyde Synthase (AASS)



A Target Enabling Package (TEP)

Gene ID / UniProt ID / EC

10157 / Q9UDR5 / 1.5.1.8, 1.5.1.9

Target Nominator

Paulo Arruda (UNICAMP, Brazil)

SGC Authors

Jola Kopec, Izabella Pena, Elzbieta Rembeza, Mark McLaughlin, Oleg Fedorov, Claire Strain-Damerell, Solenne Goubin, Sabrina MacKinnon, Nicola Burgess-Brown, Paul Brennan, Alex MacKenzie, Paulo Arruda, Wyatt W. Yue

Collaborating Authors

N/A

Target PI

Wyatt Yue (SGC Oxford)

Therapeutic Area(s)

Metabolic & Neurological disorders

Disease Relevance

Gene upstream of [ALDH7A1](#), the molecular cause of pyridoxine-dependent epilepsy (OMIM [266100](#))

Date approved by TEP Evaluation Group

2nd June 2017

Document version

Version 3

Document version date

April 2018

DOI

<https://dx.doi.org/10.5281/zenodo.1219674>

Affiliations

N/A

USEFUL LINKS



Open Targets

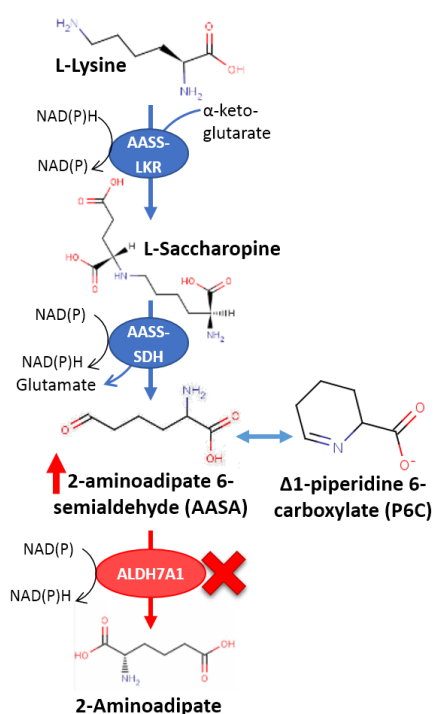


(Please note that the inclusion of links to external sites should not be taken as an endorsement of that site by the SGC in any way)

SUMMARY OF PROJECT

This work provides the early tools to develop substrate reduction inhibitors for a genetic childhood seizure disorder, with the hypothesis to target the enzyme (AASS) upstream of the defective gene (ALDH7A1) in the human lysine metabolic pathway. This TEP package includes recombinant human AASS purification protocols, structures of the AASS second domain in different states, *in vitro* assays to detect ligand binding (differential scanning fluorimetry) and enzyme activity (NADH formation) of human AASS, as well as initial chemical matters.

SCIENTIFIC BACKGROUND



Genetic linkage – Pyridoxine-dependent epilepsy (PDE) is an autosomal recessive neonatal seizure disorder, caused by inherited mutations in the *ALDH7A1* gene of the lysine metabolic pathway (1). To date, > 80 disease-causing alleles have been reported, half of which are missense changes on the encoded protein ALDH7A1 (aka antiquitin or α-aminoadipate semialdehyde dehydrogenase). A main pathogenic driver of PDE is accumulation of α-aminoadipate semialdehyde (AASA), substrate for ALDH7A1 (2), as well as its cyclic form L-Δ1-piperidine-6 carboxylate (P6C). The latter reacts with pyridoxal 5'-phosphate (PLP) thereby depleting its availability in the cell as cofactor for > 140 metabolic reactions.

Unmet need – The mainstay treatment for PDE is administration of pyridoxine, a precursor of PLP, which reduces epileptic episodes in a subset of patients. However, the delay in neurodevelopment and cognition, found in >75% of PDE patients, is not repaired by pyridoxine (3), underlying the need for alternative therapies.

Hypothesis – We propose that inhibiting the enzyme upstream of ALDH7A1, namely aminoadipate semialdehyde synthase (AASS), to reduce accumulation of AASA/P6C could serve as substrate reduction therapy for PDE (**left**).

The therapeutic rationale:

- (a) The elevated plasma and urine levels of AASA/P6C in patient cells arise predominantly from the lysine degradation pathway containing the AASS enzyme step (and not the alternative pipecolate pathway) (4);
- (b) A few reported individuals with inherited AASS mutations present a clinically benign metabolic condition (hyperlysinemia type I; (5)).

RESULTS – THE TEP

Human AASS (hAASS) is a bi-functional enzyme catalysing the first two steps in lysine catabolism (5), via its N-terminal lysine ketoglutarate reductase (LKR; EC 1.5.1.8) and C-terminal saccharopine dehydrogenase (SDH; EC 1.5.1.9) domains (**below**).



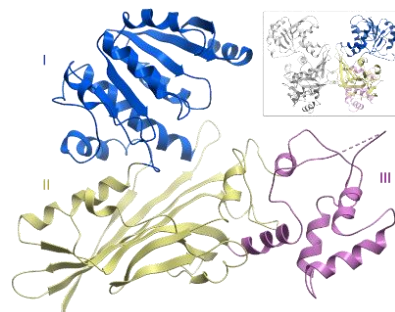
Proteins purified: hAASS LKR and SDH domains, and full-length protein

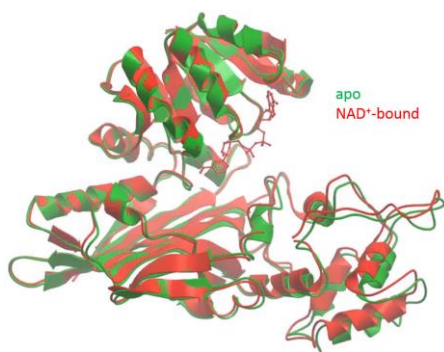
We have expressed and purified human hAASS-LKR (aa 23-452, in *E. coli*) and hAASS-SDH (aa 455-926, in insect *Sf9*) domains separately, and as near-full-length polypeptide (aa 23-926, in *E. coli*).

Structural data: hAASS-SDH domain in apo and NAD⁺-bound states

We determined the structures of hAASS-SDH in the *apo* state at 1.9 Å resolution and in binary complex with NAD⁺ at 2.7 Å resolution.

The hAASS-SDH protomer comprises three structural domains (**above**): domain I is a NAD⁺ binding Rossmann-like fold, domain II is an α/β fold responsible for substrate binding and dimerization (**above, inset**), and domain III is all-α domain regulating active site opening and closure.





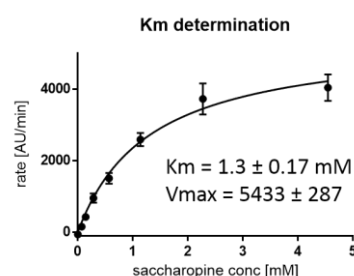
In the binary complex, NAD⁺ is bound in the Gly-rich motif of domain I. hAASS-SDH preferentially uses NAD⁺ over NADP⁺, because the anionic Asp512 and bulky Met513 side-chains preclude any possibility to accommodate a 2' ribose phosphate in NADP⁺.

The hAASS-SDH apo and binary structures superimpose with a relatively high C^α-rmsd (1.0 Å), suggesting cofactor-dependent conformational changes (**left**). We observed a 7° rigid-body rotation of domain III relative to the protein core, resulting in tightening of the active site.

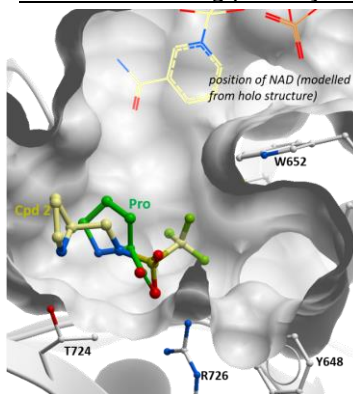
In vitro assays: differential scanning fluorimetry and fluorescence activity assay

Differential scanning fluorimetry – We adopted DSF to detect binding of native ligands, showing that the cofactor NAD⁺ alone, but not substrate saccharopine alone, causes a shift in melting temperature (ΔT_m) of 2–4°C, while substrate and cofactor together lead to a total ΔT_m of 6.5°C.

Enzyme activity – We measured hAASS-SDH activity by following the NAD⁺ reduction to NADH with fluorescence when excited at 340 nm. We confirmed *in vitro* activity for purified hAASS-SDH, yielding K_M values of 0.1 mM and 1.3 mM for NAD⁺ and saccharopine respectively (**right**).

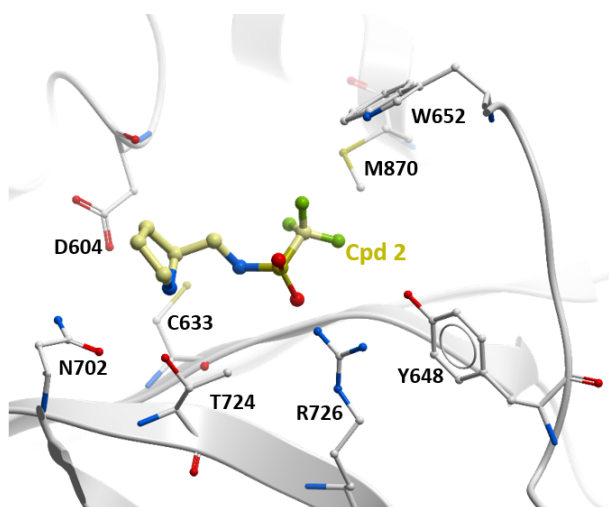
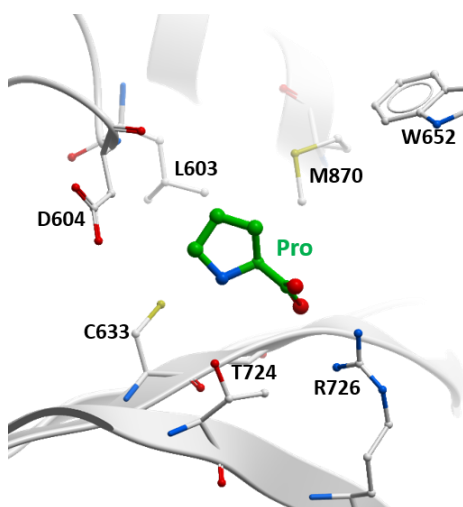


Chemical starting points from crystal soaking studies

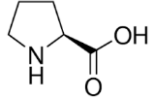
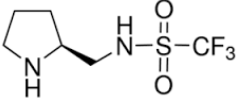
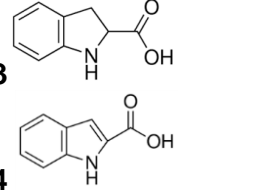
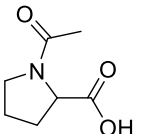
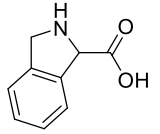


A small fragment soaking campaign by crystallography has been performed. To date we have identified a proline ligand (Pro) in the active site of hAASS-SDH:

- bound in a pocket where the substrate saccharopine is expected to bind (**left**)
- key charge interaction between proline carboxylate and invariant Arg726 at the bottom of this pocket (**below, left**)
- solution data from DSF showed that Pro caused a ΔT_m shift of 3°C to the protein



A number of commercially available proline analogues (**2-6**) has been acquired. From these, we have further determined the crystal structure bound with compound **2** within the same substrate pocket in the active site (**above, right**). Compound **2** retains a charge interaction with Arg726, but also picks up hydrogen bonds with the conserved residues Thr724 and Tyr648, as well as van der Waals interaction with Met870. Four other compounds (**3-6**) have shown inhibition of SDH activity at low mM concentrations, and will be subjected to chemistry optimization and soaking studies in future.

Bound to substrate pocket		Inhibition of activity at low mM		
 1, Proline 2.67 Å	 2 2.28 Å	 3 4	 5	 6
	Sigma 689017	Fluorochem 209339, Sigma I5109	Enamine 12587	CombiBlocks SS2281

IMPORTANT: Please note that the existence of small molecules within this TEP indicates that chemical matter can bind to the protein in a functionally relevant pocket. As such these molecules should not be used as tools for functional studies of the protein unless otherwise stated as they are not sufficiently potent or well-characterised to be used in cellular studies. The small molecule ligands are intended to be used as the basis for future chemistry optimisation to increase potency and selectivity and yield a chemical probe or lead series.

Ongoing and future work

- 1. HTS with activity assay** - Our fluorescence activity assay has been adopted and miniaturized by NIH-NCATS (*Anton Simeonov*). To date, they have carried out a pilot screen of 4625 compounds from their approved and investigational libraries (NPC, MIPE). Some hits with $IC_{50} < 10 \mu M$ have been validated by counter-screens (NADH-Glo assay, HPGD activity assay), and are also replicated in our in-house activity assay. Expanded screening of the NPACT (n=10k) and Genesis (n=100k) libraries is currently underway.
- 2. Chemistry optimisation Pro-based ligands** – Several series of compounds are being progressed, and synthesis of analogues is ongoing. Exploration of sulfonamide derivatives is of priority and a small library is currently being prepared for testing. Additionally, substitution of the proline core is being investigated, with various distinct chemotypes being assessed (*Paul Brennan, SGC-ODDI*).
- 3. Testing in patient cells and disease models** – Lead compounds from activity and crystallography based screening will be tested for their efficacy in available patient skin fibroblasts (*Philippa Mills, UC London*) as well as a PDE model in zebrafish (*Alex MacKenzie, CHEO Canada*). Data from our collaborators have provided the cellular proof-of-concept for AASS inhibition: (i) shRNA knockdown of AASS in PDE fibroblasts significantly reduced levels of toxic metabolites and rescued disease phenotypes; (ii) AASS knock down in HEK293T cells did not confer detrimental phenotypes.

Collaborations

A special thanks to our collaborators Anton Simeonov (NIH-NCATS), Paul Brennan (SGC-ODDI), Philippa Mills (UC London), and Alex MacKenzie (CHEO Canada).

CONCLUSION

Despite the first report of the aminoadipate semialdehyde synthase (AASS) gene and enzyme in the 1980s (6), three decades on, there remains a distinct lack of biochemical and structural characterization that illuminates the enzymatic properties and mechanism. The AASS TEP project and outputs therefore aim to address this gap, and importantly provide a starting point for structure-based drug design. PDE is a debilitating rare disease with an unmet medical need. With the therapeutic proof-of-concept already in place from our clinician collaborators, we aim to develop this into a translational drug discovery project as the next step, with collaborations in HT screening and validation in relevant cell lines and disease models.

FUNDING INFORMATION

The work at the SGC has been funded by a grant from the Wellcome [106169/ZZ14/Z].

ADDITIONAL INFORMATION

Structure Files

PDB ID	Structure Details
5O1P	Structure of hAASS-SDH apo
5L78	Structure of hAASS-SDH bound with NAD
5O1O	Structure of hAASS-SDH bound with Pro
5O1N	Structure of hAASS-SDH bound with N-[(2S)-2-Pyrrolidinylmethyl]-trifluoromethanesulfonamide (compound 2)

Materials and Methods

Protein expression, purification and assay procedures of hAASS-SDH

Vector: pFB-LIC-Bse

Cell line: DH10Bac

Tags and additions: N-terminal, TEV protease cleavable hexahistidine tag

Construct protein sequence:

MGHHHHHHSSGVDLGTENLYFQ*SMALPDKYKIYQTLRESRERAQSLSMGTRRKVLVLGSGYISEPVLEYLSRDGNIEITVGS
DMKNQIEQLGKKYNINPVSMICKQEEKLGFLVAKQDLVISLLPYVLHPLVAKACITNKVNMVTASYITPALKELEKSVEDAGI
TIIGELGLDPLDHMLAMESIDKAKEVGATIESYISYCGGLPAPEHSNNPLRYKFSWSPVGLMNMVMSATYLLDGKVVNVA
GGISFLDAVTSMDFFPGLNLEGYPNRDSTKYAEIYGISSAHTLLRGTLRYKGYMKALNGFVKLGLINREALPAFRPEANPLTWK
QLLCDLVGISPSSEHDVLKEAVLKKLGGDNTQLEAAEWLGLLGDEQVPQAESILDALSKHLVMKLSYGPEEKDMIVMRDSFGI
RHPSGHLHKTIDLVAYGDIINGFSAMAKTVGLPTAMAAKMLLDGEIGAKGLMGPFSEKIYGPILERIKAEGIIYTTQSTIKP
(underlined sequence contains vector encoded His-tag and TEV protease cleavage site*)

Bacmid DNA was prepared from DH10Bac cells and used to transfect Sf9 insect cells for the preparation of initial baculovirus. [AASS](#) protein was expressed from infected Sf9 cells cultivated in InsectXpress medium (Lonza) for 72 hours at 27°C.

Harvested cells were resuspended in lysis buffer (50 mM HEPES pH 7.4, 500 mM NaCl, 5% Glycerol, 20 mM Imidazole pH 7.4, 0.5 mM TCEP, 1 µL per 1 mL protease inhibitor cocktail EDTA-free).

Cell pellet was dissolved in approximately 200 mL lysis buffer and broken by homogenization by 2 passes at 12,000 psi. The cell debris was pelleted at 35000 x g, 1h and the supernatant used for purification on a gravity flow Ni-NTA column (5 mL).

Buffers used are detailed hereafter;

Binding Buffer: 50 mM HEPES pH 7.4, 500 mM NaCl, 5% Glycerol, 20 mM Imidazole pH 7.4, 0.5 mM TCEP

Wash Buffer: 50 mM HEPES pH 7.4, 500 mM NaCl, 5% Glycerol, 40 mM Imidazole pH 7.4, 0.5 mM TCEP

Elution Buffer: 50 mM HEPES pH 7.4, 500 mM NaCl, 5% Glycerol, 250 mM Imidazole pH 7.4, 0.5 mM TCEP

The clarified cell extract was added to 5 ml of Ni-NTA resin pre-equilibrated with lysis buffer and passed through a glass column. The column was then washed with Binding Buffer (2 x 50 mL) and Wash Buffer (2 x 50 mL). The protein was eluted with Elution Buffer in 5 x 5 mL fractions. The eluted fractions from column 1 were pooled and concentrated to 5 mL with a 30 kDa MWCO spin concentrator and injected into an S200 16/60 column (pre-equilibrated in GF Buffer (50 mM HEPES pH 7.4, 500 mM NaCl, 0.5 mM TCEP, 5% Glycerol)) at 1.0 mL/min. 1.5 mL-fractions were collected. The eluted protein was cleaved overnight at 4 °C by TEV protease (1/20 (w/w)). The following day protein sample was loaded onto 0.5ml Ni-sepharose column pre-equilibrated with GF buffer to remove uncleaved protein. Pooled protein fractions were concentrated to 13 mg/mL using a 30 kDa mwco concentrator.

Activity assay and screening

The SDH activity of hAASS was measured by following NAD⁺ reduction to NADH, taking advantage that the reduced form of NADH is fluorescent when excited with 340 nm light. We adopted the assay into 384-well format, with detection using the PheraStar fluorescence reader (BMG Labtech) (Excitation/Emission = 340/480 nm). This assay gave a linear response with protein concentration up to 150 nM. A typical reaction consists of 100 nM purified enzyme, 0.2 mM NAD⁺, 1.3 mM saccharopine. The reaction buffer consists of 25 mM HEPES pH 7.4, 100 mM NaCl, 0.1% BSA, 0.05% CHAPS. The compound libraries (LOPAC (Sigma) and NIH Clinical Collections I&II) were screened in-house at 20 µM compound concentration.

Differential scanning fluorimetry

DSF was performed in a 96-well plate using an Mx3005p RT-PCR machine (Stratagene) with excitation and emission filters of 492 and 610 nm, respectively. Each well consisted of 2 µL protein in 2 µM DSF buffer (150 mM NaCl, 10 mM HEPES pH 7.5), 2 µL SYPRO ORANGE diluted 1000-fold in DSF buffer from the manufacturers stock (Invitrogen), and (if applicable) 2 µL ligand at various concentrations. Fluorescence intensities were measured from 25 to 96°C with a ramp rate of 3°C/min.

Crystallization

Apo crystals were prepared by mixing 50 nL of hAASS-SDH protein (80 mg/mL) with 100 nL of reservoir solution containing 20% PEG3350, 0.1M Tris pH 7.5 and 0.2-0.33 M sodium malonate. NAD⁺-bound crystals were prepared by mixing 100 nL of hAASS-SDH (18 mg/mL, in molar excess of NAD⁺) with 50 nL of reservoir solution containing 25% PEG3350, 0.2M NaCl and 0.1M tris pH 8.5. Crystals were cryo-protected in 9% butanediol before freezing in liquid nitrogen. For the fragment screening campaign, crystals were soaked with compounds (10/50/500 mM) in the crystallization solution supplemented with 8% butanediol for 5-30 min, and frozen in liquid nitrogen.

Structure determination procedures

hAASS-SDH apo and NAD⁺-bound crystals belong to different spacegroups (P43212 vs P212121). The structure of hAASS-SDH was solved by molecular replacement with the program PHASER, using the fungal saccharopine reductase from *S.cerevisiae* (PDB code 2AXQ) as search model (38% sequence identity). Two molecules were found in the asymmetric unit (a.u.). The initial model was rebuilt using phenix.autobuild. A bound NAD⁺ molecule in the active site was identified by difference Fourier method and manually placed into the electron density using Coot. To complete the model iterative cycles of phenix.refine including TLS refinement followed by manual model building for missing residues using coot were performed. No NCS restraints were applied due to conformational differences in domain III (res 278-376) of the two copies in the a.u. Solvent atoms were placed during the last four rounds of refinement using phenix.refine. For the fragment screening campaign, ligands were identified by DIMPLE (<https://github.com/ccp4/dimple>) using difference density maps. Weaker binders with low occupancy were evaluated using PANDDA (<https://pandda.bitbucket.io/>), based on statistical models to find ligand density present in a given dataset that is not present in majority of datasets. Coordinates and structure factors for all data sets are deposited in the RCSB Protein Data Bank. Data collection and refinement statistics are available from the PDB pages.

Commercially available reagents

CRISPR/Cas9 knockout plasmids
SCBT: Cat # sc-406408
Genscript: Cat # 10157

References

1. Mills, P. B., Struys, E., Jakobs, C., Plecko, B., Baxter, P., Baumgartner, M., Willemsen, M. A., Omran, H., Tacke, U., Uhlenberg, B., Weschke, B., and Clayton, P. T. (2006) [Mutations in antiquitin in individuals with pyridoxine-dependent seizures](#). *Nat Med* **12**, 307-309
2. Brocker, C., Lassen, N., Estey, T., Pappa, A., Cantore, M., Orlova, V. V., Chavakis, T., Kavanagh, K. L., Oppermann, U., and Vasiliou, V. (2010) [Aldehyde dehydrogenase 7A1 \(ALDH7A1\) is a novel enzyme involved in cellular defense against hyperosmotic stress](#). *The Journal of biological chemistry* **285**, 18452-18463
3. van Karnebeek, C. D., Tiebout, S. A., Niermeijer, J., Poll-The, B. T., Ghani, A., Coughlin, C. R., 2nd, Van Hove, J. L., Richter, J. W., Christen, H. J., Gallagher, R., Hartmann, H., and Stockler-Ipsiroglu, S. (2016) [Pyridoxine-Dependent Epilepsy: An Expanding Clinical Spectrum](#). *Pediatr Neurol* **59**, 6-12
4. Pena, I. A., Marques, L. A., Laranjeira, A. B., Yunes, J. A., Eberlin, M. N., MacKenzie, A., and Arruda, P. (2017) [Mouse lysine catabolism to aminoadipate occurs primarily through the saccharopine pathway; implications for pyridoxine dependent epilepsy \(PDE\)](#). *Biochim Biophys Acta* **1863**, 121-128
5. Houten, S. M., Te Brinke, H., Denis, S., Ruiter, J. P., Knecht, A. C., de Klerk, J. B., Augoustides-Savvopoulou, P., Haberle, J., Baumgartner, M. R., Coskun, T., Zschocke, J., Sass, J. O., Poll-The, B. T., Wanders, R. J., and Duran, M. (2013) [Genetic basis of hyperlysinemia](#). *Orphanet J Rare Dis* **8**, 57
6. Markovitz, P. J., Chuang, D. T., and Cox, R. P. (1984) [Familial hyperlysinemias. Purification and characterization of the bifunctional aminoadipic semialdehyde synthase with lysine-ketoglutarate reductase and saccharopine dehydrogenase activities](#). *The Journal of biological chemistry* **259**, 11643-11646